

# Morphological and infra-red studies on highly oriented poly(vinylidene fluoride)/poly(methyl methacrylate) blends

W. Kaufmann and J. Petermann

*Technical University of Hamburg-Harburg, Polymer and Composites Group, Hamburg, FRG*

N. Reynolds, E. L. Thomas and S. L. Hsu\*

*Polymer Science and Engineering Department, University of Massachusetts, Amherst, Massachusetts, USA*

*(Received 5 December 1988; accepted 19 January 1989)*

Highly oriented melt drawn films of poly(vinylidene fluoride) (PVDF) and blends of poly(vinylidene fluoride) and poly(methyl methacrylate) (PMMA) have been studied by transmission electron microscopy, electron diffraction and infra-red spectroscopy. Infra-red spectra show the second moment of the orientation function for PVDF samples to be greater than 0.94. Using such a sample, the transition dipole directions relative to the chain axis have been calculated. Electron microscopic studies of the PVDF/PMMA blends show a transformation for pure PVDF from a lamellar morphology to a mixture of lamellar and needle-like crystals for the 80/20 blend. The 60/40 blend shows a pure needle-like morphology. The  $\beta$  phase content for this blend is dependent upon the composition and thermal history. An increase in the  $\beta$  phase content is observed with the addition of PMMA. After annealing at 110°C, the 50/50 blend shows a lamellar  $\beta$  phase morphology. A significant increase in the segmental orientation of PVDF is also observed.

(Keywords: morphology; blends; infra-red spectroscopy; poly(vinylidene fluoride); poly(methyl methacrylate))

## INTRODUCTION

Poly(vinylidene fluoride) (PVDF) may crystallize into at least five different crystalline phases<sup>1</sup>. The most common one is the  $\alpha$  phase crystallized at high degrees of supercooling. The piezoelectric  $\beta$  phase usually can only be obtained at low degrees of supercooling<sup>2</sup>. Blends of PVDF with poly(methyl methacrylate) (PMMA) are miscible in the molten phase<sup>3-12</sup>. It is known that the relative amounts of the  $\alpha$  and  $\beta$  phases of PVDF and the size and orientation of different crystallites all vary significantly with the blend composition and crystallization conditions<sup>13-15</sup>. The  $\beta$  phase of PVDF, however, is difficult to obtain unless the samples are crystallized under unusual conditions, such as under high pressure, on external substrates, or in the presence of a high external electrical field<sup>2,16</sup>. In our previous studies, it was demonstrated that the  $\beta$  phase of PVDF can be successfully obtained when crystallized in a high longitudinal flow gradient<sup>15,17-19</sup>. For blends of PVDF with PMMA, the  $\beta$  phase content is increased under these conditions<sup>15</sup>.

Infra-red activity is insensitive to long-range order or disorder, but is sensitive to order on the angstrom scale, whereas TEM and electron diffraction provide information on larger scale structure. Thus vibrational spectroscopy and TEM and electron diffraction provide complementary structural information. When transition dipole moments of individual vibrations are well defined, infra-red dichroism measurements provide a measure of the overall chain orientation. By comparing the dichroic behaviour of bands assigned to crystalline and amorphous regions, we can determine the orientation of both

components. Our primary goal of the current study is to correlate the large-scale molecular structure and morphology measured by TEM and electron diffraction to the local molecular structure measured by infra-red spectroscopy. The phase content, morphology and chain orientation of PVDF are monitored as a function of blend composition. The effects of annealing on these factors are also examined.

## EXPERIMENTAL

PVDF samples were obtained from the Daikin Kogyo Corp., Japan, and the PMMA ( $M_n=60\,000$ ,  $M_w=120\,000$ ) was Plexiglas-Formmasse 8N supplied by Rohm GmbH, West Germany. Both components were dissolved in the appropriate weight fractions (100/0, 80/20, 60/40 and 50/50 PVDF/PMMA) in a common solvent (cyclohexanone). Extremely thin films approximately 100 nm thick were prepared according to the method of Petermann and Gohil, which provides a high extensional flow gradient during crystallization and large supercooling<sup>20</sup>. The melt draw temperatures for the various compositions were 150, 141, 131 and 125°C, respectively. These films were studied directly by electron diffraction and TEM experiments. Both Philips 400T and JEOL 100CX electron microscopes were employed for the morphological investigations.

Polarized infra-red spectra were obtained with a Bruker IFS 113v FTi.r. spectrometer. Samples 10 layers thick were used for infra-red and thermal analysis. These films were obtained by wrapping the film around the glass slide during drawing. Free-standing films were obtained by floating the films onto water from the glass

\* To whom correspondence should be addressed

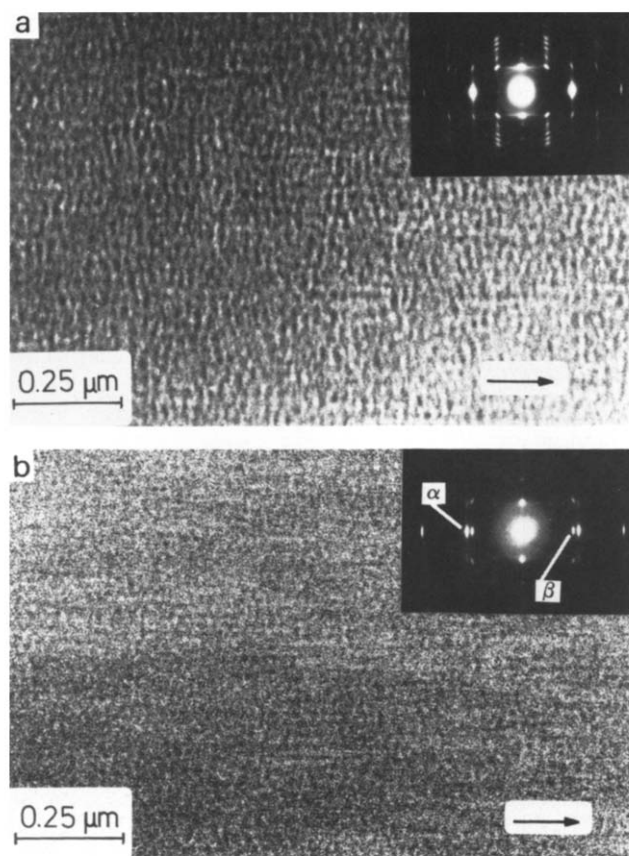


**Figure 1** (a) TEM phase-contrast bright-field micrograph of the 100% PVDF sample. The molecular direction is indicated by the arrow. The vertical grey ribbons represent the crystalline lamellae; the brighter parts are the amorphous layers. Inserted is an electron diffraction pattern of the sample showing oriented  $\alpha$  phase. (b) TEM micrograph of 80% PVDF/20% PMMA. A mixture of lamellar and needle-like morphology is seen. The inserted electron diffraction shows the (0 0 2)  $\alpha$  and (0 0 1)  $\beta$  reflections

substrate. A wire-grid polarizer was used to obtain polarized radiation. For such thin films, generally 1000 scans at  $2\text{ cm}^{-1}$  resolution were collected in order to obtain high signal-to-noise ratio.

Samples were annealed under tension between 100 and  $110^\circ\text{C}$  for 10 min. This temperature range is below the onset of premelting, as determined by a Heraeus DTA 500 with a d.s.c. measuring cell, operating at a heating rate of  $10\text{ K min}^{-1}$ .

## RESULTS AND DISCUSSION

Figures 1a and 1b show TEM phase-contrast bright-field micrographs of films containing 100% and 80% PVDF, respectively. Figures 2a,b and 3a,b show the data obtained for blends containing 60% and 50% PVDF, respectively. The corresponding electron diffraction patterns are inserted. As reported earlier<sup>15,19</sup> a transformation from a lamellar morphology (pure PVDF) to a mixed morphology containing lamellar and needle-like crystals in the 80% PVDF/20% PMMA blend, then into a pure needle-like morphology in the 60% PVDF/40% PMMA blend is observed. From the electron diffraction patterns a qualitative picture of the molecular orientation associated with the PVDF crystals can be estimated from the angular misorientation of the diffraction spots. For both compositions, the PVDF crystals are aligned nearly

perfectly with their molecular axis parallel to the drawing direction. As we will demonstrate, infra-red data will show PMMA and PVDF chains to be oriented.

The content of the  $\alpha$  and  $\beta$  phases can be best estimated from the intensities of the (0 0 2)  $\alpha$  and (0 0 1)  $\beta$  reflections in the electron diffraction patterns. No  $\beta$  modification can be seen for the pure PVDF; however, in some regions a few micrometres away in the same sample a weak (0 0 1)  $\beta$  reflection can sometimes be observed. It has been established by the electron diffraction and infra-red results of Thomas and Yang that the  $\beta$  content in the sample increases with increasing PMMA content up to a concentration of 70% PVDF/30% PMMA<sup>15</sup>. However, in contrast to their results, no  $\gamma$  modification is detected in our samples by electron diffraction.

These qualitative results concerning overall molecular orientation and the phase contents can be considerably improved with quantitative infra-red measurements, since additional information about local chain conformations, orientation of the amorphous PVDF and PMMA, and the relative amounts of the crystal phases can all be obtained. Preliminary infra-red analysis has been performed on PVDF/PMMA blends to monitor the amount of  $\beta$  phase with blend composition and deformation<sup>15</sup>. Polarized infra-red spectra of the melt-drawn PVDF and 80% PVDF/20% PMMA blend are shown in Figures 4a,b and 5a,b, respectively. In Figure 6 are shown polarized spectra for the 50/50 blend before and after annealing at  $100^\circ\text{C}$ .

From the spectra in Figure 4 it is clear that the PVDF

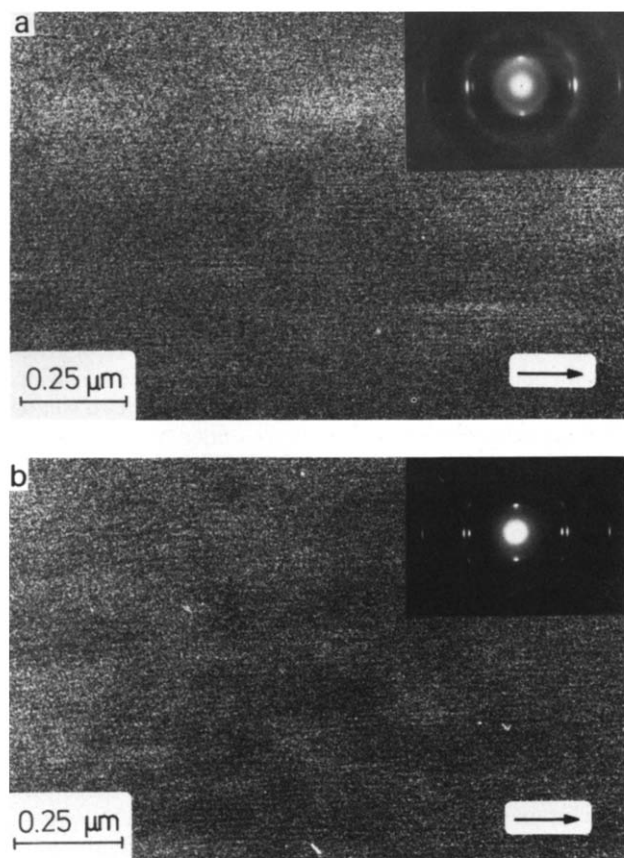


**Figure 2** (a) TEM micrograph of 60% PVDF/40% PMMA as drawn showing needle-like  $\beta$  morphology. (b) TEM micrograph of 60% PVDF/40% PMMA, annealed at  $110^\circ\text{C}$  for 10 min. Inset diffraction pattern shows an increase in the  $\beta$  phase content from the (0 0 1) reflection

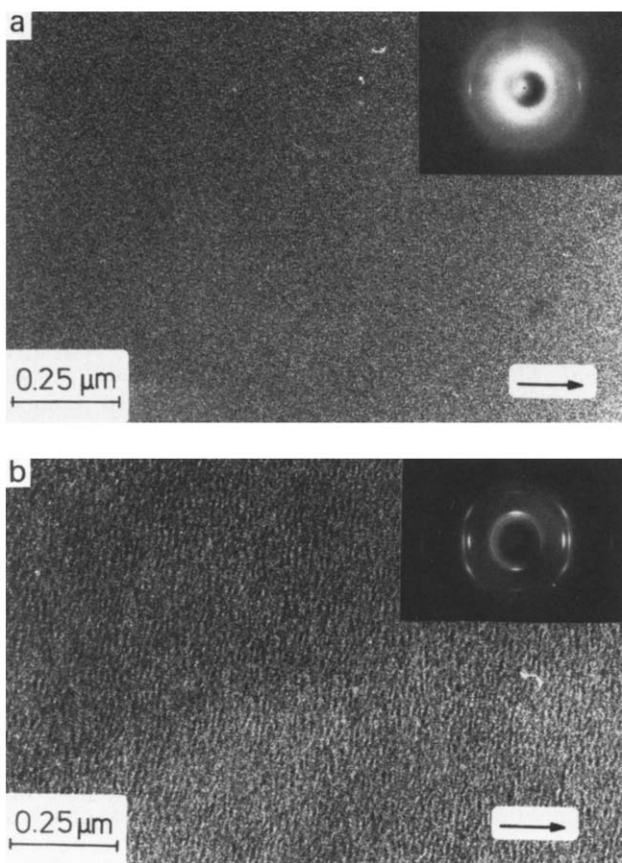


**Figure 3** (a) TEM micrograph of 50% PVDF/50% PMMA as drawn showing no ordered structure. Inset diffraction pattern shows a faint (001)  $\beta$  reflection oriented along the draw direction in an otherwise amorphous pattern. (b) TEM micrograph of 50% PVDF/50% PMMA, annealed at 110°C for 10 min. Inset diffraction pattern shows highly oriented lamellar  $\beta$  phase

film is very highly oriented. This is demonstrated by several bands such as the 976  $\text{cm}^{-1}$   $\alpha$  phase band which appears strongly with perpendicular polarization and is nearly extinct in the parallel polarized spectrum. This sample shows a degree of orientation greater than that of any other sample we have seen over the years. The relative amounts of the  $\alpha$  and  $\beta$  phases can be determined from the relative intensities of the 510  $\text{cm}^{-1}$  ( $\beta$  or  $\gamma$ ) and 530  $\text{cm}^{-1}$  ( $\alpha$ ) bands, as has been performed in earlier studies<sup>15,21</sup>. These bands have been assigned to the  $\text{CF}_2$  bending mode for the two phases<sup>22</sup>, and assuming that they have equivalent extinction coefficients, as done previously<sup>21</sup>, allows us to calculate the  $\alpha$  phase content to be 62%. A list of bands analysed, along with assignments, measured dichroic ratios and calculated transition dipole moment angles for PVDF is given in Table 1. A perpendicular polarized band is observed at 1233  $\text{cm}^{-1}$  and has been found by Kobayashi *et al.* to be associated with amorphous regions<sup>22</sup>. The strong perpendicular polarization observed for this band suggests that the amorphous regions of PVDF are also oriented in this material.

Owing to the extremely high degree of orientation of the PVDF film as determined by electron diffraction and polarized i.r. we can calculate the direction of transition dipole moments with respect to the chain axis with an initial assumption of perfect orientation. The second moment of the orientation function is described by the

following relationship:

$$f = \frac{(R_0 + 2)(R - 1)}{(R_0 - 1)(R + 2)} \quad (1)$$

where  $R$  is the dichroic ratio  $A_{\parallel}/A_{\perp}$ , and  $R_0$  is the dichroic ratio for a perfectly oriented sample calculated from

$$R_0 = 2 \cot^2 \alpha \quad (2)$$

where  $\alpha$  is the angle that the transition dipole moment makes with the chain axis. For the 976  $\text{cm}^{-1}$  band, a chain orientation function value of 0.936 is the lowest from which a positive  $R_0$  value may be determined. This then gives us a lower limit for the degree of chain orientation. The effect of infra-red beam divergence and the possibility of misalignment of the film layers are factors that would only reduce the observed dichroism. Therefore we conclude that within experimental error the second moment of the orientation function is greater than 0.94. Further analysis to determine the transition moments of various vibrations will be included in a future report.

The infra-red spectrum of an 80% PVDF/20% PMMA blend is shown in Figure 5. Again the high orientation of the PVDF is clearly visible. From the very weak dichroism observed for the 1727  $\text{cm}^{-1}$  carbonyl stretching band, we find that the PMMA shows relatively low degree of orientation as expected since these chains will relax at the high drawing temperature employed. Similar to the electron diffraction data, a lower  $\alpha$  content is

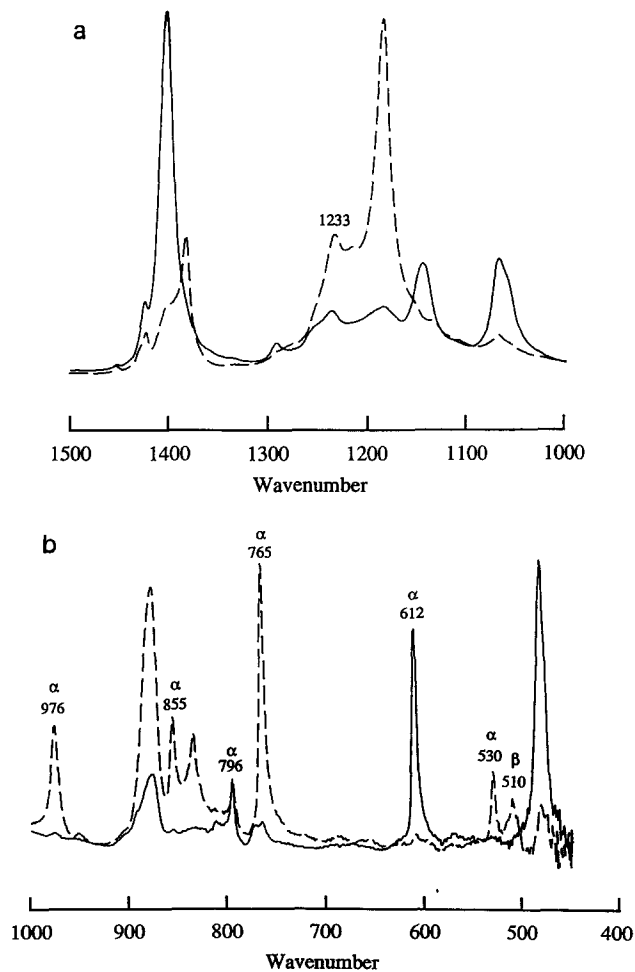


**Figure 4** Polarized infra-red spectra of drawn PVDF film: (a) 1500–1000  $\text{cm}^{-1}$  region; (b) 1000–400  $\text{cm}^{-1}$  region; (---) perpendicular polarization; (—) parallel polarization

observed (42%  $\alpha$ ) as compared to pure PVDF. No definitive conclusions about the degree of orientation of the amorphous PVDF can be made for the blends, as PMMA exhibits absorptions that overlap the  $1233\text{ cm}^{-1}$  amorphous PVDF band.

The degree of morphological change with annealing is dependent upon blend composition. For the 80/20 blend, no changes in phase content are observed upon annealing at  $100^\circ\text{C}$  for 10 min. This is not true for samples having PMMA contents of 40% and more. Figures 2a and 2b are TEM micrographs with inserted diffraction patterns of 60% PVDF/40% PMMA, as prepared (2a) and after annealing for 10 min at  $110^\circ\text{C}$  (2b). While the needle-like morphology is still maintained, the relative amount of the  $\beta$  phase increases after annealing. In a blend of 50% PVDF/50% PMMA (Figure 3a) the overall crystalline content of  $\alpha$  and  $\beta$  phases in the sample is very small as

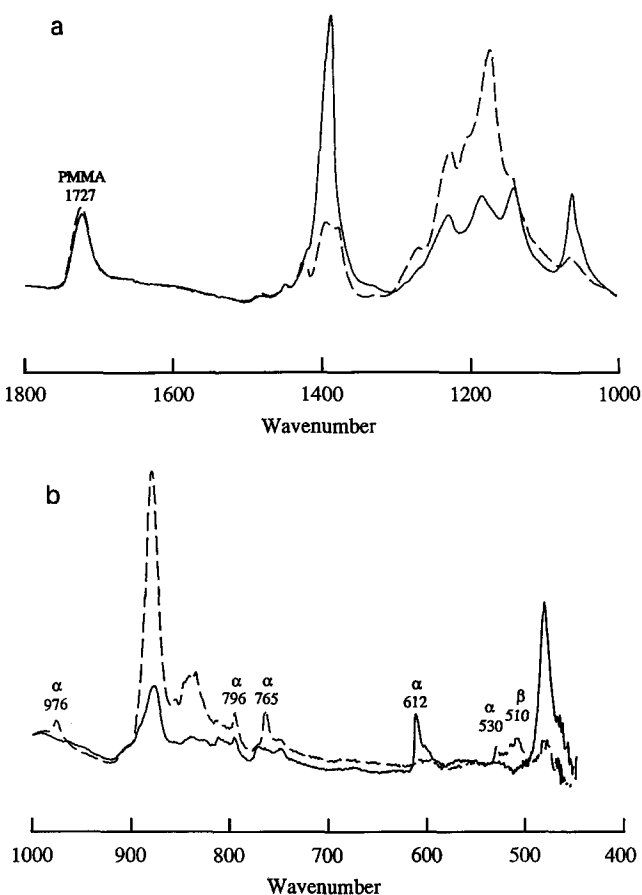


Figure 5 Polarized infra-red spectra of 80% PVDF/20% PMMA blend: (a)  $1800\text{--}1000\text{ cm}^{-1}$  region; (b)  $1000\text{--}400\text{ cm}^{-1}$  region; (—) perpendicular polarization; (---) parallel polarization

estimated from the diffraction pattern. No ordered structure at all can be seen in the TEM micrograph. Upon annealing, a distinct lamellar morphology develops consisting primarily of  $\beta$  crystals.

Infra-red spectra of the 50% PVDF/50% PMMA blend are shown in Figure 6. The infra-red bands of PVDF in this sample appear to be much less dichroic and thus chains are less oriented than for pure PVDF or the 80/20 blend. There is no clear evidence for the presence of  $\alpha$  phase in the as-drawn 50/50 blend, since neither the  $530\text{ cm}^{-1}$  nor the  $612\text{ cm}^{-1}$  bands are present. A  $510\text{ cm}^{-1}$  *trans* conformation band is only very weakly present. This is consistent with the electron diffraction pattern, which shows a tiny amount of oriented  $\beta$  phase with no significant orientation of the amorphous phase haloes. Upon annealing, an increase in the  $510\text{ cm}^{-1}$  band intensity is observed. Therefore, as also seen in the electron diffraction pattern, annealing the amorphous blend results in the direct formation of oriented  $\beta$  phase. Intensity increases in other  $\beta$  phase bands found at  $1177\text{ cm}^{-1}$  ( $\text{CF}_2$  asymmetric stretching and  $\text{CF}_2$  and  $\text{CH}_2$  rocking) and at  $840\text{ cm}^{-1}$  ( $\text{CF}_2$  symmetric stretching)<sup>11</sup> upon annealing provide further evidence for the formation of  $\beta$  phase.

Another interesting observation is the increase in the dichroism in the PVDF found upon annealing the 50/50 blend. This is clearly seen in all the PVDF bands, especially the  $1403\text{ cm}^{-1}$  ( $\text{CH}_2$  wagging and asymmetric skeletal stretching) and the  $840\text{ cm}^{-1}$  bands. After annealing we observe a slight decrease in the dichroism of the  $750\text{ cm}^{-1}$  and  $2953\text{ cm}^{-1}$  bands of PMMA. To evaluate the orientation of the amorphous PMMA, a transition moment angle of  $90^\circ$  is assumed for the  $2953\text{ cm}^{-1}$  methyl asymmetric stretching band. The second moment of the orientation function has a value of 0.116, which decreases to 0.066 upon annealing as relaxation occurs.

It is expected that  $\beta$ -phase PVDF can preferentially crystallize from the oriented amorphous 50/50 blend (Figures 3a and 3b). However, it is interesting that there is an increase in PVDF chain orientation during annealing for this blend as well. The increased orientation of the PVDF may be accomplished by a reptational propagation of 'kinks' of the PVDF chain within a 'tube' comprising PMMA chains and nucleation and growth of  $\beta$ -PVDF crystals. If the crystallization is diffusion-controlled, the fastest diffusing chain segments will form the nucleus. At constant 'tube' diameter, chain segments with the largest amount of *trans* isomers will be the fastest diffusing, because their width compared to the 'tube' diameter is smallest, and this, consequently, favours the all-*trans* chain conformation of the  $\beta$ -PVDF crystal. Additionally, the orientation of PMMA molecules will cause rather

Table 1 Dichroic ratios, transition dipole moment directions and band assignments for  $\alpha$ -PVDF

Wavenumber	Dichroic ratio ( $A_{\parallel}/A_{\perp}$ )	Transition moment angle, $\alpha$ (deg)		Band assignment <sup>21</sup>
		$f=1$	$f=0.94$	
976	$\perp$ 0.044	81.6	86.0	$\text{CH}_2$ t <sup>a</sup> (82%)
855	$\perp$ 0.140	75.2	76.9	$\text{CH}_2$ r (48%)
796	$\parallel$ 0.988	54.9	54.9	$\text{CH}_2$ r (78%)
765	$\perp$ 0.096	77.7	79.9	$\text{CF}_2$ $\delta$ (33%), CCC $\delta$ (21%)
612	$\parallel$ 14.307	20.5	17.9	$\text{CF}_2$ $\delta$ (24%), CCC $\delta$ (19%)

<sup>a</sup> t, twisting; r, rocking;  $\delta$ , bending

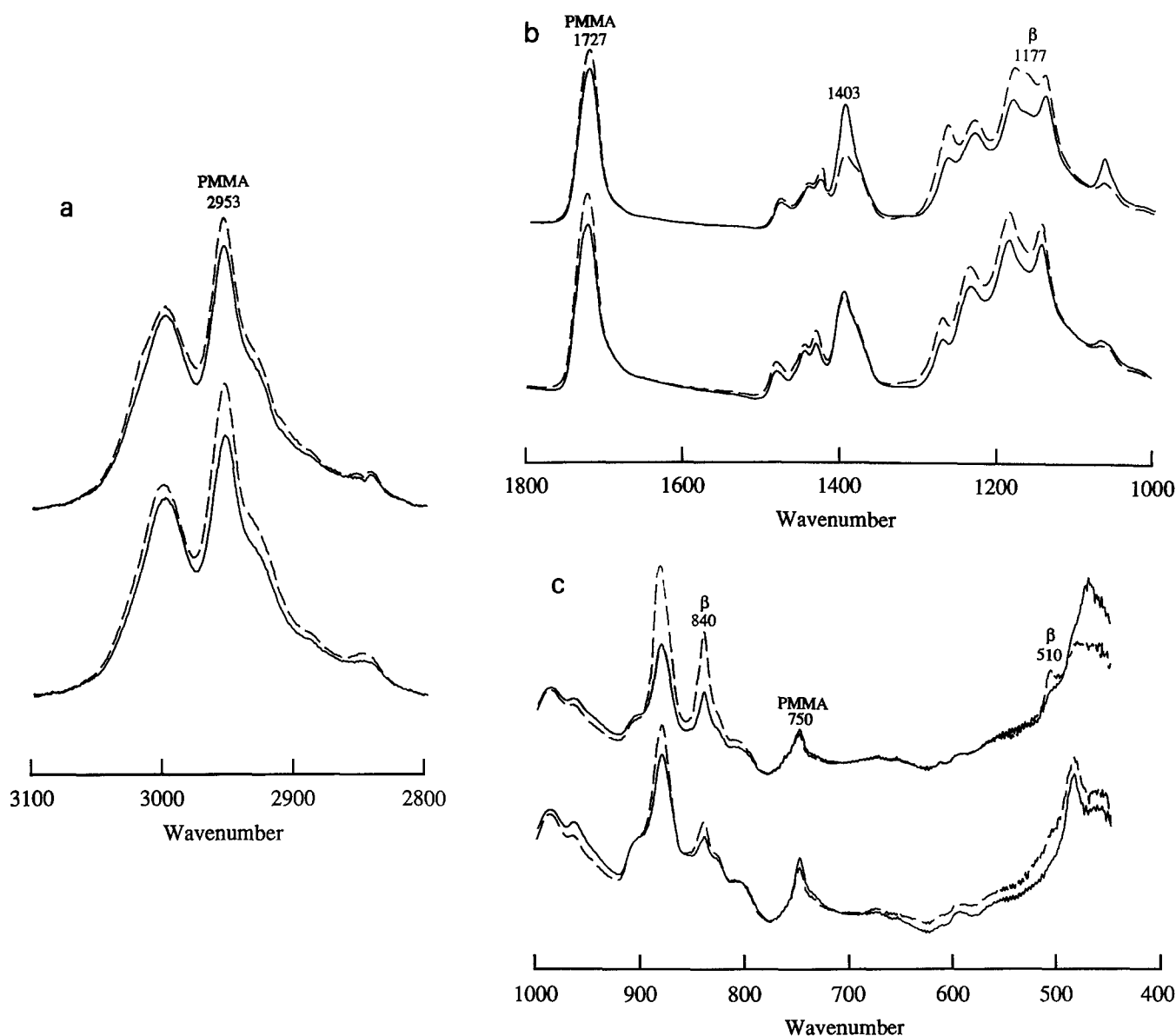


**Figure 6** Polarized infra-red spectra of 50% PVDF/50% PMMA blend: (a) 3100–2800  $\text{cm}^{-1}$  region; (b) 1800–1000  $\text{cm}^{-1}$  region; (c) 1000–400  $\text{cm}^{-1}$  region; (—) perpendicular polarization; (—) parallel polarization; (bottom) as drawn; (top) after annealing at 100°C

straight 'tubes' and increase the number of *trans* segments of the diffusing PVDF chain. Hence, the crystallization of  $\beta$ -PVDF from oriented amorphous PVDF/PMMA blends is consistent with a diffusion-controlled mechanism. The occurrence of diffusion-controlled crystallization has already been suggested by Yang and Thomas<sup>15</sup>, and the crystallization of  $\beta$ -PVDF from blends having very high PMMA contents has also been reported by several authors<sup>13,14</sup>, but no explanation has been offered for its occurrence as yet. The increase in segmental dichroism during crystallization of the  $\beta$ -PVDF within this blend can be understood from the formation of the crystal nucleus in the molecular orientation direction and the decrease of *gauche* conformations by subsequent crystallization.

In conclusion, we found that both the localized structures measurable by infra-red spectroscopy and morphological features measurable by TEM and electron diffraction differ significantly depending on blend composition or annealing conditions. Melt-drawn PVDF films are highly oriented with the second moment of the

orientation function found to be greater than 0.94. As previously reported, an increase in  $\beta$  phase content is observed with the addition of PMMA (62%  $\alpha$  in PVDF and 58%  $\beta$  in the 80/20 blend), as well as a morphological change from a lamellar structure to a mixture of lamellar and needle-like crystals with reduced orientation for the 80/20 blend. A pure needle-like morphology is observed for the 60/40 blend. The 50/50 blend shows a weakly oriented amorphous structure. Annealing at 100°C for 10 min produces highly oriented lamellar  $\beta$  phase along with a slight reduction of the PMMA orientation.

#### ACKNOWLEDGEMENTS

One of the authors (J.P.) acknowledges the support of the Institute for Interface Science supported by a grant from IBM during his research stay at the University of Massachusetts. This research is supported by a grant from the National Science Foundation, Polymers Program, Grant No. DMR-8407539.

REFERENCES

- 1 Lovinger, A. J. *Science* 1983, **220**, 1116
- 2 Lovinger, A. J. 'Developments in Crystalline Polymers' (Ed. D. C. Bassett), Applied Science, London, 1982, p. 195
- 3 Noland, J. S., Hsu, N. N. C., Saxon, R. and Schmitt, J. M. *Adv. Chem. Ser.* 1971, **99**, 15
- 4 Nishi, T. and Wang, T. T. *Macromolecules* 1975, **8**, 909
- 5 Paul, D. R. and Altamirano, J. O. *Adv. Chem. Ser.* 1975, **142**, 371
- 6 Coleman, M. M., Zarian, J., Varnell, D. F. and Painter, P. C. *J. Polym. Sci., Polym. Lett. Edn.* 1977, **15**, 745
- 7 Hourston, D. J. and Hughes, J. D. *Polymer* 1977, **18**, 1175
- 8 Paul, D. R., Barlow, J. W., Bernstein, R. E. and Wahrmund, D. R. *Polym. Eng. Sci.* 1978, **18**, 1225
- 9 Roerdink, E. and Challa, G. *Polymer* 1978, **19**, 173
- 10 Roerdink, E. and Challa, G. *Polymer* 1980, **21**, 509
- 11 Wendorff, J. H. *J. Polym. Sci., Polym. Lett. Edn.* 1980, **18**, 439
- 12 Morra, B. S. and Stein, R. S. *J. Polym. Sci., Polym. Phys. Edn.* 1982, **20**, 2243
- 13 Morra, B. S. and Stein, R. S. *J. Polym. Sci., Polym. Phys. Edn.* 1982, **20**, 2261
- 14 Leonard, C., Halary, J. L., Monnerie, L., Broussoux, D., Servet, B. and Micheron, F. *Polym. Commun.* 1983, **24**, 110
- 15 Yang, D. and Thomas, E. L. *J. Mater. Sci. Lett.* 1987, **6**, 593
- 16 Lu, F. J. and Hsu, S. L. *Macromolecules* 1986, **19**, 326
- 17 Gohil, R. M. and Petermann, J. *Polymer* 1981, **22**, 1612
- 18 Yang, D. C. and Thomas, E. L. *J. Mater. Sci.* 1984, **3**, 929
- 19 Hausler, E., Kaufmann, W., Petermann, J. and Stein, L. *Ferroelectrics* 1984, **60**, 45
- 20 Petermann, J. and Gohil, R. M. *J. Mater. Sci.* 1979, **14**, 2260
- 21 Hsu, S. L., Lu, F. J., Waldman, D. A. and Muthukumar, M. *Macromolecules* 1985, **18**, 2583
- 22 Kobayashi, M., Tashiro, K. and Tadokoro, H. *Macromolecules* 1975, **8**, 158